

ARTICLE TEMPLATE

Efficient STIRAP-like scheme for coherent population transfer by revisited optimal control theoryAmine Jaouadi^a and Mamadou Ndong^{b,c}^aQatar Foundation, Tornado Tower, Floor 5, PO. Box 5825, Doha, Qatar; ^bLaboratoire de Physique de l'Université de Bourgogne, UMR 5027 CNRS et Université de Bourgogne, BP 47870, 21078 Dijon, France; ^cCollège Evariste Galois, Unité d'enseignement secondaire, 13 Rue Jean Giraudoux, 95200 Sarcelles, France**ARTICLE HISTORY**

Compiled June 16, 2019

ABSTRACT

We demonstrate that Optimal Control Theory (OCT) with a state-dependent constraint which depends on the state of the system at each instant can reproduce the famous counterintuitive mechanism of Stimulated Raman adiabatic passage (STIRAP). We examine this behavior in a Λ -type three-level system and we show that could be applied for sequentially coupled many-level systems. We study the robustness of the two methods with respect to pulse fluctuations and the decays. We show that new OCT formulation appears to be more robust than STIRAP when a perturbation is introduced in the pulses. Such method is of great use for systems involving coherence loss such as molecular systems with dissociation or ionization limits. It also may find potential applications in the control of chemical reactions, quantum optics, and quantum information processing.

KEYWORDS

STIRAP; Coherent population transfer; Laser; Optimal control theory

1. Introduction

The problems of coherent control and efficient population transfer between atomic or molecular levels have been given plenty of attention and prominence both theoretically and experimentally (1–11) over the past few decades. They represent a great interest for a number of applications such as quantum computing, optical control of chemical reactions, spectroscopy and collision dynamics. STIRAP (2, 12) has proven to be a robust technique to ensure an almost complete level-to-level population transfer. This transfer scheme results from a mechanism involving a counterintuitive sequence of two laser pulses, conventionally called the pump and the Stokes pulses. The counterintuitive behavior is translated by an unforeseen phenomena that the Stokes pulse, which is applied in a second time, precedes and overlaps the pump pulse.

Many studies have been carried out on the processes of STIRAP (3, 4, 13). According to the literature, STIRAP-type solution from Local Control Theory (LCT) has been already demonstrated (14, 15). Compared to LCT, the optimal control theory (OCT) appears to be more flexible and more efficient, particularly, for complex

systems with many degrees of freedom. In fact, OCT requires information only about the initial and the final (target) states. Hence, to find the optimal field leading to the desired objective, OCT adopts the most appropriate route using a forward-backward iteration process. However, LCT needs information at every instant during the optimization cycle in order to ensure a monotonic increment in the sought objective. By using OCT, Yuan et al. (16) have proposed an analytical derivation of a STIRAP-type solution for specific many-level systems in a peculiar framework, by assuming that the Rabi frequency is not bounded. The “*new*” variant of OCT formulated with state-dependent constraint (17) has been used by Müller et al. (18) for the purpose to simulate quantum gates within polar molecules and neutral atoms systems. By coincidence, the authors have observed a STIRAP-like solution when analyzing the optimized fields.

We show in this paper that by using a state-dependent constraint, the counterintuitive scheme generated from STIRAP can indeed be achieved. We compare here the efficiency of STIRAP and the new OCT by analyzing the robustness with respect to the decay and with respect to the pulse fluctuations. Finally, we demonstrate that OCT with state-dependent constraint can be extended to many-level systems.

The paper is organized as follows. In section 2, we give a brief overview of STIRAP and the results obtained from the Λ -type three-level system. In section 3, we first, illustrate that standard OCT can not reproduce the counterintuitive scheme. Secondly, we demonstrate that the new OCT with state-dependent constraint leads in an automatic fashion to such a mechanism. Then, we compare the robustness of the new OCT method against STIRAP with respect to the decay and to pulses fluctuations. Before concluding we show that the new OCT method can be extended for multilevel systems. And finally we conclude in section 4.

2. STIRAP

We consider the interaction of two laser pulses with the Λ -type three-level system shown in Fig. 1. The levels are sequentially coupled two-by-two: the levels $|1\rangle$ and $|2\rangle$ are coupled by the first field Ω_p , which conventionally we call the pump pulse and the levels $|2\rangle$ and $|3\rangle$ are coupled by the second field Ω_s usually called the Stokes. The transition between levels $|1\rangle$ and $|3\rangle$ is electric-dipole forbidden. Δ represents the detuning of the intermediate level $|2\rangle$. We suppose as an initial condition that only level $|1\rangle$ is populated and the durations of the pump and the Stokes are shorter than the relaxation times of the system. We remind here that the ultimate goal of STIRAP is to transfer, in a efficient way, all the population from the initial state $|1\rangle$ to the final state $|3\rangle$ with minimum loss in the intermediate level $|2\rangle$. This has been studied intensively over the past few decades. However, to achieve this goal STIRAP has to go through a peculiar mechanism, which is manifested by the counterintuitive sequence of the two laser pulses. The Stokes pulse arrives before the pump pulse although initially we apply the pump pulse before the Stokes. The dynamics of the three-level system are described by the following time-dependent Schrödinger equation:

$$i\frac{d}{dt}a(t) = \hat{H}(t)a(t). \quad (1)$$

Where $a(t) = [a_1(t), a_2(t), a_3(t)]^T$, $a_1(t)$, $a_2(t)$ and $a_3(t)$ are respectively the probability amplitudes of the states $|1\rangle$, $|2\rangle$, and $|3\rangle$.

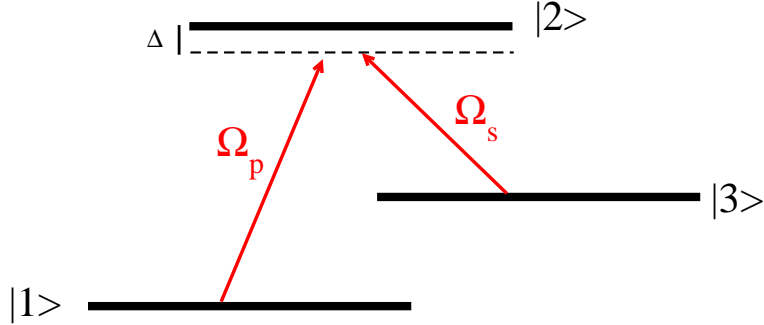


Figure 1. Schematic energy level diagram of the Λ -type three-level system. Levels $|1\rangle$ and $|2\rangle$ are coupled by the pump laser Ω_p . Levels $|2\rangle$ and $|3\rangle$ are coupled by the Stokes laser Ω_s . Δ represents the detuning of the intermediate level $|2\rangle$.

Using the rotating-wave approximation, the time-dependent Hamiltonian \hat{H} of the system can simply be written as:

$$\hat{H}(t) = \begin{bmatrix} 0 & \Omega_p(t) & 0 \\ \Omega_p(t) & \Delta(t) & \Omega_s(t) \\ 0 & \Omega_s(t) & 0 \end{bmatrix}. \quad (2)$$

Where $\Omega_p(t)$ and $\Omega_s(t)$ represent the Rabi frequencies of the two pulses. Indexes p and s refer to the pump and the Stokes pulses respectively.

In Fig. 2, we display the dynamics of the populations as a function of time. We choose a period $T = 100$ fs as a duration for both pulses. At time $t = T$, STIRAP leads to an almost a complete transfer of population from state $|1\rangle$ (the dashed green curve) to state $|3\rangle$ (the solid dark curve). However, as one can notice in Fig. 2(a) level $|2\rangle$ (the dotted red curve) is not completely dark. For comparative purposes with other methods presented in the following section, we analyze in detail the population being remained in the intermediate level $|2\rangle$. In Fig. 2(b), we show a zoom of the population of the state $|2\rangle$ as a function of time (red dotted curve). We observe that the population has to go through a peak at around $t \simeq 45$ fs where it reaches a maximum of $\simeq 0.8\%$. It is well known that STIRAP generates automatically a counterintuitive and unanticipated behavior, where we found once the process is over, the Stokes pulse is followed by the pump pulse. Again for purpose of comparison, we plot in Fig. 3 the pulses generated by STIRAP for a pulse duration $T = 100$ fs. We can observe that the counterintuitive sequence of Stokes pulse (in dashed red curve) followed by the pump pulse (solid black curve) emerges clearly as it was expected (4).

3. Optimal Control Theory

In this section we first investigate the standard OCT method applied to the three-level Λ system. Where the aim is the same: ensure to transfer the whole population from the initial state $|1\rangle$ to the target state $|3\rangle$ without or with minimum of dissipation through the intermediate state $|2\rangle$. Subsequently, we analyze the implementation of state-dependent constraint developed by Palao et al. (17) in order to achieve efficient and complete population transfer. We then, study the robustness of the new OCT method and compare it to STIRAP performance. Finally, we show that the new OCT with the state-dependent constraint can be extended for systems involving more than

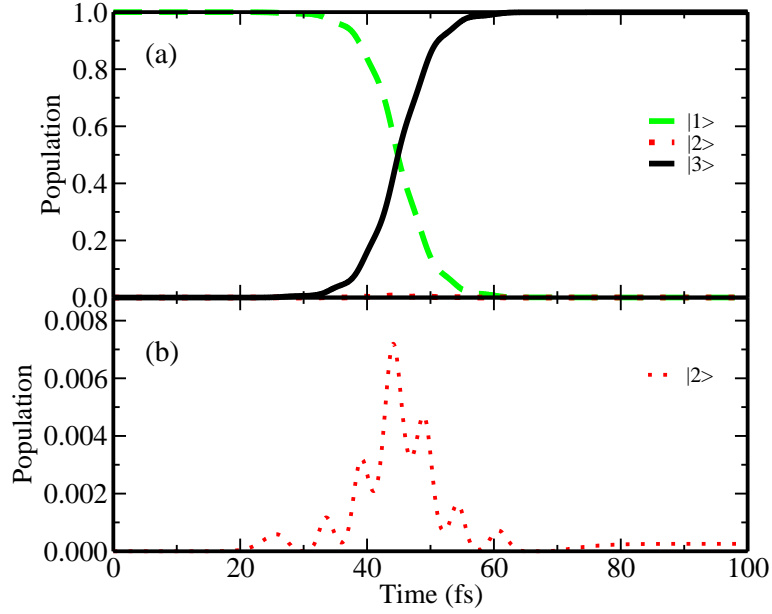


Figure 2. The time evolution of the population in the three states with laser parameters generated by STIRAP. Level $|1\rangle$ is presented in green dashed line, level $|2\rangle$ in red dotted line, and level $|3\rangle$ in solid dark line.

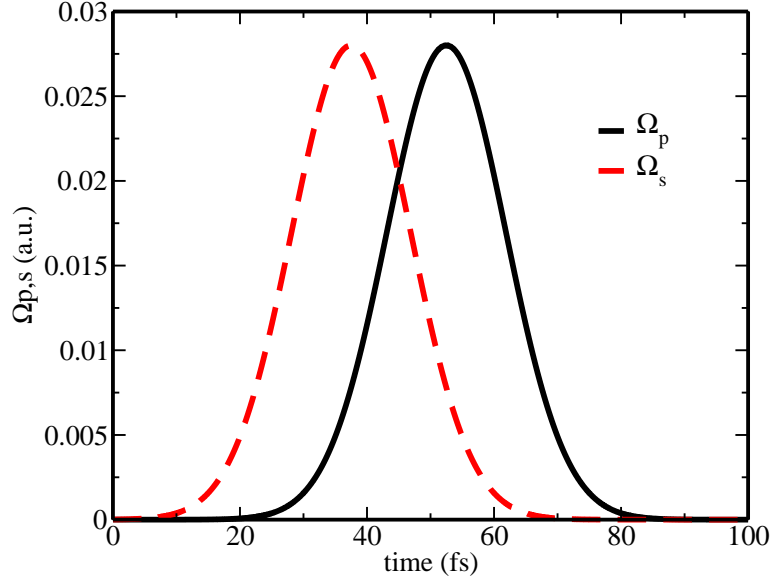


Figure 3. The sequence of the two pulses produced by using STIRAP method. We note that the counterintuitive sequence is generated automatically; the Stokes pulse (dashed red line) precedes the pump pulse (solid dark line).

three levels.

3.1. OCT Standard Method

Generally, in the implementation of an OCT scheme, as a general rule, one would like to drive the system from an initial state to a specified target state at the final time. Usually the optimization requires to define an objective functional J , which has to be

maximized or minimized (19, 20).

Here, we first formulate briefly the basics of optimal control theory for the Λ -type three-level system. The objective is to find the optimal laser field that drives the system from the initial state $|\varphi_i\rangle = |1\rangle$ to the target state $|\varphi_f\rangle = |3\rangle$ at the final time T .

In such case the functional J is written as the following:

$$J_{\text{st}} = |\langle \Psi_i(T) | \varphi_f \rangle|^2 - \int_0^T \lambda_a(E(t) - E_{\text{ref}})^2 dt, \quad (3)$$

where the index st refers to the standard OCT method. $E(t)$ denotes the electric field and E_{ref} is the reference field. The optimization could be carried out only within a specific time frame $[0, T]$. The first term in Eq. (3) represents the objective or the yield. It serves to measure the quality of the control, it may, inter alia, overlaps with the target state $|\varphi_f\rangle$ (present case) or determine an expected value for an hermitian operator. The role of the second term is to limit the laser energy through the penalty factor $\lambda_a(t) = \lambda_0/S(t)$, where $S(t) = \sin^2(\pi t/T)$. It constraints the intensity of the laser to not exceed a certain limit, called the Keldysh limit (21).

Maximizing the objective functional Eq. (3) can be achieved by resolving numerically a system of three coupled equations (22): The Schrödinger equation for $|\Psi_i(t)\rangle$ with initial condition $|\Psi_i(t=0)\rangle = |\varphi_i\rangle$ (conventionally called forward propagation), the Schrödinger equation for the Lagrange multiplier with a final condition $|\Psi_f(t=T)\rangle = |\varphi_f\rangle$ (conventionally called backward propagation), in addition to an equation for the optimal field. The system of equations to be resolved can be written as the following:

$$\frac{\partial}{\partial t} |\Psi_f(t)\rangle = -i\hat{H}|\Psi_f(t)\rangle, \quad |\Psi_f(T)\rangle = |\varphi_f\rangle, \quad (4a)$$

$$\frac{\partial}{\partial t} |\Psi_i(t)\rangle = -i\hat{H}|\Psi_i(t)\rangle, \quad |\Psi_i(t=0)\rangle = |\varphi_i\rangle, \quad (4b)$$

$$E(t) = E_{\text{ref}}(t) + \Delta E(t) \quad (4c)$$

$$\Delta E(t) = \frac{S(t)}{\lambda_a} \Im(\langle \Psi_f(t) | \hat{\mu} | \Psi_i(t) \rangle).$$

Where $\hat{\mu}$ represent the dipole coupling. In order to resolve these coupled equations different methods have been proposed (22, 23) in the past. For instance, the Krotov method involves rather an iterative procedure which, simultaneously, leads to the maximization of the functional at the end of the process. We therefore use Krotov method in our study. In fact, this method needs to adjust the field over the time towards a monotonic convergence in a self-consistent way. Further details on how Krotov method operates could be found in (23, 25, 26). Our purpose here is to demonstrate that the standard OCT method cannot lead to a proper coherent population transfer in the three-level system shown in Fig. 1. For a same pulse duration $T = 100$ fs as in STIRAP example, we display the populations evolution as a function of time in Fig. 4. We can see in Fig. 4(a) that standard OCT leads to a transfer of population from state $|1\rangle$ represented here in green dashed line to state $|3\rangle$ represented by the solid black line. However this transfer could not be coherent, where we notice in Fig. 4 (b) a big population amount had to go through the intermediate state $|2\rangle$ represented by the dotted red line. We notice that around $\simeq 50\%$ of the population reside in state $|2\rangle$ at $t = 50$ fs. Figure. 5 shows the natural intuitive feature that occurs when we adopt the standard OCT method. The pump pulse presented in solid dark curve is clearly followed by the Stokes pulse presented in red dashed curve. In fact, this behavior is the

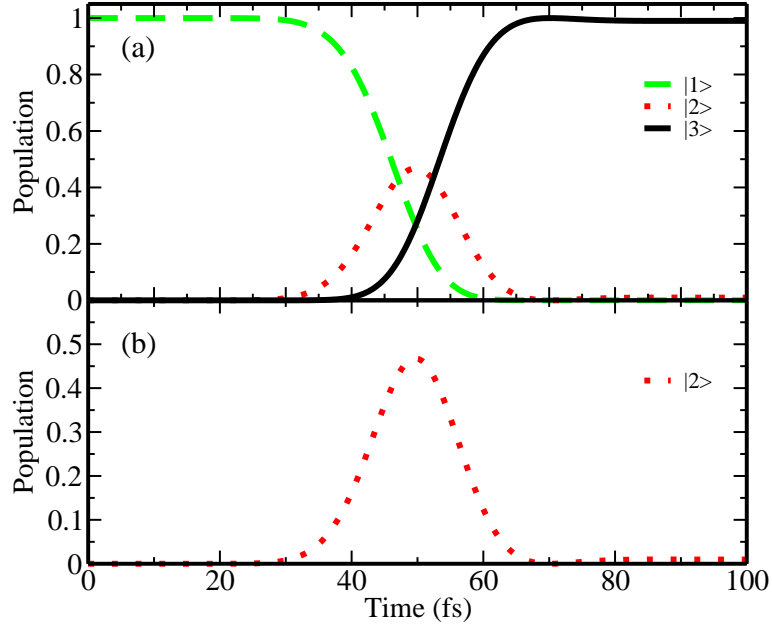


Figure 4. The time evolution of the population in the three states $|1\rangle$ (green dashed line), $|2\rangle$ (dotted red line), and $|3\rangle$ (solid black line) with laser parameters generated by the standard OCT method.

expected one since as initial conditions we apply the pump pulse before the Stokes.

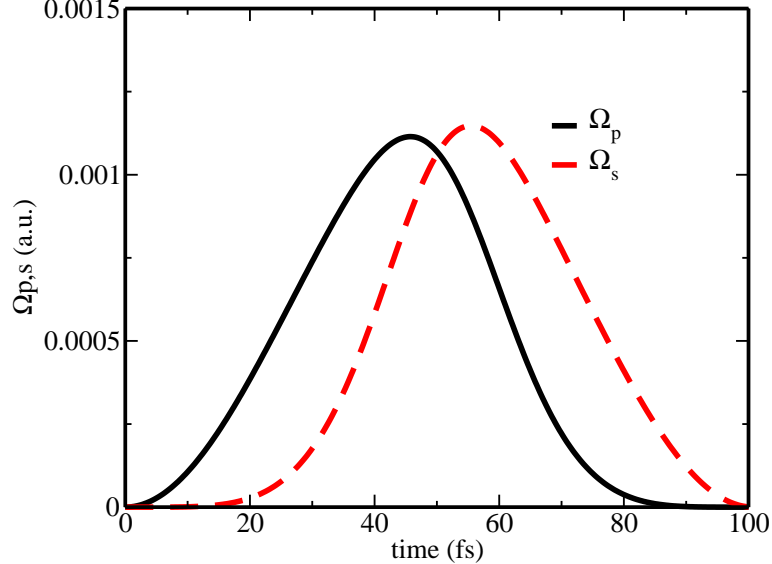


Figure 5. The sequence of the two optimized pulses obtained using the standard OCT method. We note that the intuitive sequence of pump pulse (solid dark curve) followed by Stokes pulse (red dashed curve) is generated automatically

3.2. OCT with State-Dependent Constraint

In reference (14) it was clearly mentioned that “*Without robustness being incorporated explicitly into the objective functional in OCT there is no reason to expect STIRAP-type solutions to emerge from OCT calculation*”. Here we point out that the state-

dependent constraint included into the objective functional (17) leads to this kind of particular solution where the counterintuitive scheme is plainly visible.

By introducing the state-dependent constraint within the objective functional Eq. (3), one could obtain:

$$J_{\text{new}} = J_{\text{st}} + \underbrace{\lambda_b \int_0^T \langle \Psi_i(t) | \hat{D} | \Psi_i(t) \rangle dt}_{\text{state-constraint}}; \quad (5)$$

with $\hat{D} = |1\rangle\langle 1| + |3\rangle\langle 3|$. The second term of Eq. (5) describes the state-dependent constraint. The objective of the optimization herein consists of avoiding population transfer to level $|2\rangle$. As defined by Palao et al. (17), here the states $|1\rangle$ and $|3\rangle$ form the allowed subspace. Contrariwise state $|2\rangle$ corresponds to the forbidden subspace. The optimization can be achieved by solving the three couple equations Eq. (4). However the equation of backward propagation, Eq. (4a), should be modified in order take into account the state-dependent constraint. Therefore, we obtain the following equation which has to be resolved along with other equations of the system by using the same technique adopted in standard OCT method.

$$\frac{\partial}{\partial t} |\Psi_f(t)\rangle = -i\hat{H}|\Psi_f(t)\rangle + \lambda_b \hat{D}|\varphi(t)\rangle, \quad |\Psi_f(T)\rangle = \varphi_f. \quad (6)$$

Eq. (6) is solved numerically by using a Chebychev propagator for inhomogeneous Schrödinger equation (24). Figure 6(a) shows the time evolution of the population in

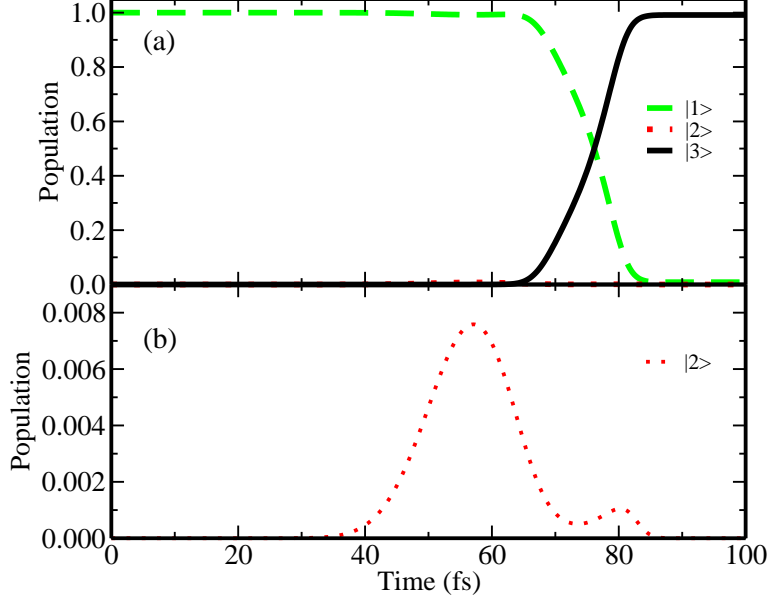


Figure 6. The time evolution of the population in the three states $|1\rangle$ (green dashed line), $|2\rangle$ (red dotted line), and $|3\rangle$ (dark solid line) with laser parameters generated by the new OCT method with state-dependent constraint.

the three-level system generated by the new OCT method with the state-dependent constraint. One can observe a better population transfer from level $|1\rangle$ presented in green dashed line to level $|3\rangle$ presented in dark solid line. In order to examine the

efficiency of this transfer, the population in the intermediate level $|2\rangle$ which has been locked in the objective functional is shown in Fig 6(b). One could see that the time evolution of population in level $|2\rangle$ attains its maximum of 0.75% at $t = 59$ fs. Then the population completely vanished at the end of the pulse. This result reveals to be more interesting compared to the result obtained from the local optimization. One could notice in Fig.7 of (15) that the population in level $|2\rangle$ has a higher value around 1% and keeps have the same over its time evolution until the pulse is off. In addition compared to the standard OCT method, the population transfer is enhanced significantly indeed. The amount of the population went through the level $|2\rangle$ with the standard OCT method was around 50%, and yet we have less than 0.75% in same level with the new OCT method.

Furthermore, in Fig. 7 we display the optimized pulses obtained by the new OCT method. Although, we do not obtain the same envelope for both pulses, we see fairly that the Stokes presented in dashed red line precedes and overlaps the pump presented in solid dark line. We thus retrieve the counterintuitive feature of STIRAP in a systematic manner.

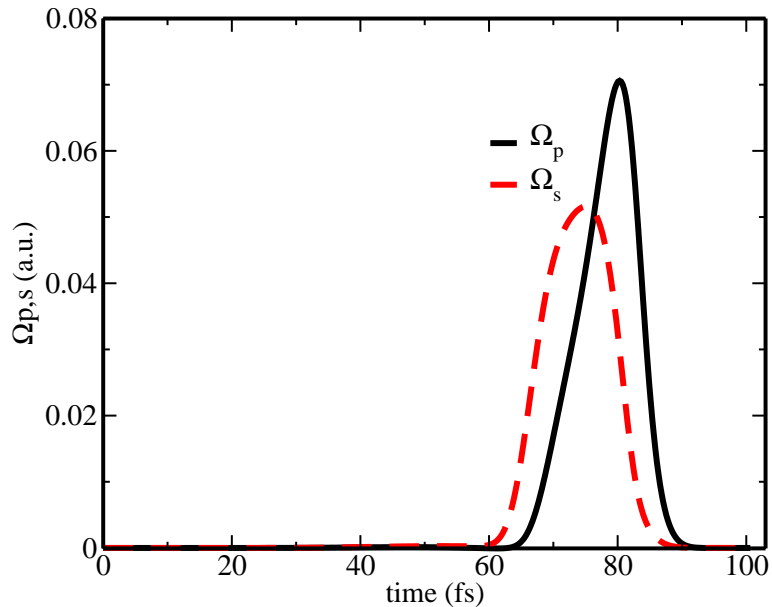


Figure 7. The sequence of the two optimized pulses obtained using the new optimal control theory method with state-dependent constraint. We distinctly see the counterintuitive sequence of Stokes pulse (red dashed line) followed by pump pulse (solid dark line) is generated automatically as in STIRAP method.

3.3. Comparison of Robustness

So far we have shown that the new OCT technique can produce the counterintuitive scheme as in STIRAP method. Here, we analyze the robustness of these two method with respect to the pulse fluctuations and the decay of the intermediate state $|2\rangle$. Firstly, we introduce fluctuations in the optimized pluses by adopting the following technique:

$$\Omega'_{s,p}(t) = \Omega_{s,p}(t) + \alpha\zeta(t), \quad (7)$$

where $\Omega_{s,p}(t)$ is the solution obtained by the new OCT or STIRAP. Indexes s and p refer respectively to the Stokes and pump pulses. $\zeta(t)$ is the perturbation function modeled by a vector of random numbers chosen within the interval $[-1, 1]$ and α is a factor parameter.

Secondly, in order to investigate the robustness of the two methods with respect to the decay, we introduce a simple loss mechanism in level $|2\rangle$. For the obvious reason that the goal of STIRAP scheme in a three-level system is to transfer the population from level $|1\rangle$ to level $|3\rangle$ (see Fig. 1) by minimizing the population of the intermediate level $|2\rangle$. This loss mechanism could be modeled by adding an imaginary term $-i\beta\Gamma$ to the energy of the level $|2\rangle$, where $\Gamma = 1/T$ represents the decay rate and β is a second factor parameter.

Consequently the corresponding new Hamiltonian becomes:

$$H' = \begin{bmatrix} 0 & \Omega'_p(t) & 0 \\ \Omega'_p(t) & \Delta - i\beta\Gamma & \Omega'_s(t) \\ 0 & \Omega'_s(t) & 0 \end{bmatrix}. \quad (8)$$

We then solve the Schrödinger equation using the new Hamiltonian given in Eq. (8). We analyze separately the robustness, firstly with respect to the pulse fluctuations and secondly with respect to the decay. In our analysis, the amplitude of the Rabi frequencies of the STIRAP approach is chosen in a way that the condition for adiabatic following is fulfilled. This condition is given in Ref. (2) by $\Omega_{s,p}^{\max}\tau \gg 10$ with τ the time overlap of the two Rabi frequencies and $\Omega_{s,p}^{\max}$ the maximum of the Rabi frequency. The upper panel of Fig. 8 compares the robustness between the STIRAP and the new

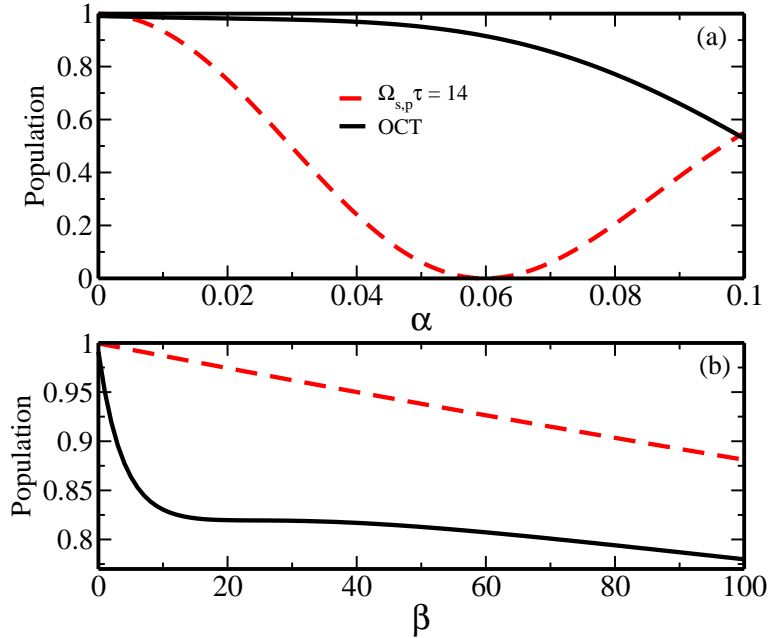


Figure 8. Population at final time in the target level $|3\rangle$ induced by the Hamiltonian of Eq. (8). In the upper panel, β parameter in Eq. (8) is set to 0 while in the lower panel $\alpha = 0$. The dashed red curve shows the results obtained with the STIRAP method and the solid black curve represents the results obtained with the new OCT approach.

OCT approach with respect to the pulse fluctuations. While the lower panel of Fig. 8 compares the robustness of these two methods with respect to the decay introduced

in Eq. (8). The figure displays the population at the final instant of the target level $|3\rangle$ as a function of α parameter (Fig. 8(a)) or β parameter (Fig. 8(b)). In addition to the adiabatic following condition, for the results shown in Fig. 8, we ensured that the energy of the STIRAP field is set to be equivalent to the energy of the optimized field generated by the new OCT method. Since in the STIRAP approach are defined analytically, one expect that this method would be more robust. But surprisingly, it is clearly seen from the solid black line of the upper panel of Fig. 8 that the new OCT method is less sensitive to the field perturbation than the STIRAP approach. Once a field perturbation is introduced, the dashed red line that describes the results obtained with the STIRAP decreases drastically. For example for $\alpha = 0.06$, the population in the target state is only about 2% for the STIRAP method while it is greater than 90% for new OCT method. The fact that the optimized pulses are more robust than the ones produced by STIRAP with regards to the pulse fluctuations is attributed to the pulses duration. In fact the FWHM of the optimized pulses is two times shorter than the STIRAP pulses.

Contrariwise in the lower panel of Fig. 8 we observe an opposite behavior. The STIRAP method appears to be more robust with respect to the decay. The dashed red curve shows a linear decrease of the population. For instance, when $\beta = 100$, the population in the target state is about 87% for the STIRAP method. The solid black curve which displays the results obtained with new OCT method shows an exponential decrease when $0 \leq \beta \leq 10$. At $\beta = 100$, the population in the target state is about 78% for the new OCT method. Hence, at first glance, one could conclude that the robustness of each of these methods depends on what we take into consideration which is usually dictated by the experiment setup. In order to investigate more the robustness and

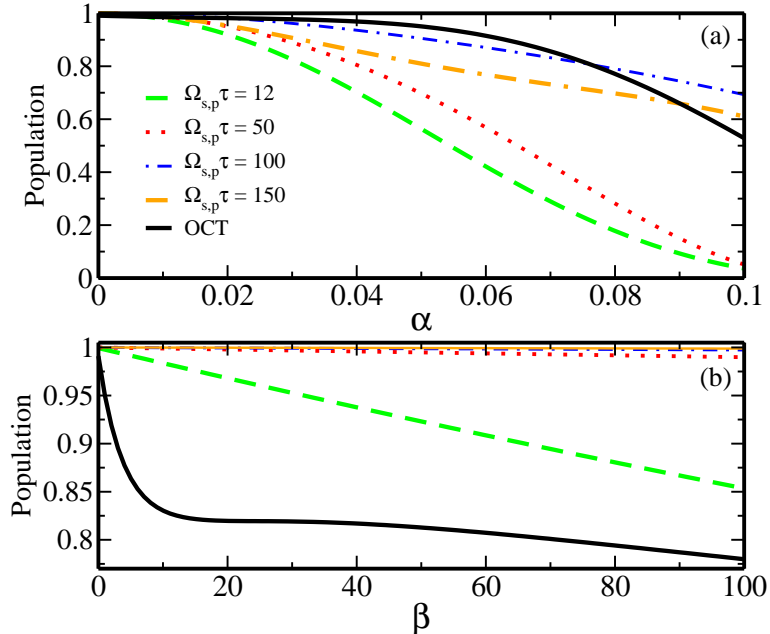


Figure 9. Same as in Fig. 8. Comparison of robustness for several field energies of the STIRAP method.

going further in respecting the adiabatic following condition $\Omega_{s,p}^{\max}\tau \gg 10$, we show in figure 9 the same comparison as in Fig. 8 the population of the target state when the pulse is off, yet for different field energies of the STIRAP pulse. In panel (a), the results corresponding to $\Omega\tau = 100$ and $\Omega\tau = 150$ show that the robustness of the

STIRAP with respect to the pulse fluctuations does not necessarily increase when we increase the field energy as one could expect. However the efficiency with regard to the decay is significantly improved when we increase the energy of the initial pulse, Fig. 8(a). Yet we should emphasize on two points here, regarding the efficiency as a function of the decay, indeed STIRAP appears to be more robust, however the new OCT still keep having high population within the target state, the minimum value is 78% when $\beta = 100$, in addition to the fact that we did not increase the energy of the initial pulse for OCT. The second point is about the adiabatic following condition, it is of course very important to fulfill this condition to ensure a population transfer within STIRAP. However it implies to choose higher energies for the initial pulses, which usually represents a kind of burden for experimental setups. This analysis allows us to conclude that, for the population transfer from an initial state to a final one, the OCT method with the state-dependent constraint is more robust than the STIRAP when perturbations are introduced in the field. However STIRAP is more efficient when we refer to the decay in the intermediate state of the system.

3.4. Many-level system

One of the major results of reference (14) is the general applicability of LCT. It was shown that LCT can be straightforward implemented for N-level systems to reproduce STIRAP scheme. By using a STIRAP pulses sequence, LCT led to a population transfer within four- and nine-level systems. We show here that OCT with the state-dependent constraint can be extended to multilevel systems as well, and lead to a cor
vel
wn
vel
in

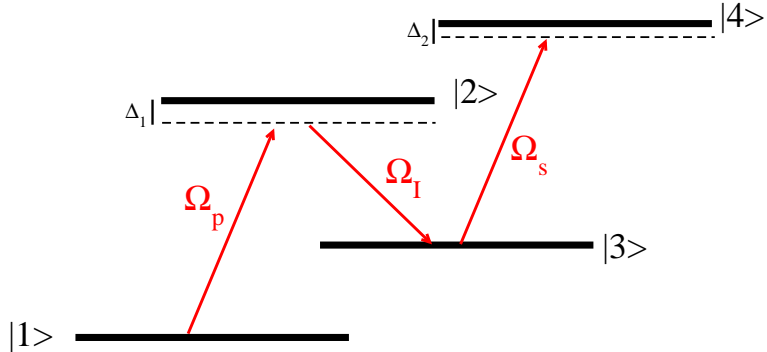


Figure 10. A four-level system with sequential couplings. Level $|1\rangle$ and $|2\rangle$ are coupled by a field with amplitude Ω_p . Levels $|2\rangle$ and $|3\rangle$ are coupled by a field with amplitude Ω_I and levels $|3\rangle$ and $|4\rangle$ are coupled by a field with amplitude Ω_s . Δ_1 and Δ_2 are respectively the detuning of levels $|2\rangle$ and $|4\rangle$.

system. In similar fashion, the process of the transfer from the initial state $|1\rangle$, presented in dashed green curve, to the target state $|4\rangle$, presented in solid black curve, is analogue to the one in the Λ -type three-level system. We obtain indeed an almost complete population transfer. In Fig 11(b), we focus on the two intermediate states $|2\rangle$ (dotted red line) and $|3\rangle$ (dot-dashed blue line) in order to examine the quality of the transfer. One can see that the percentages of population passed through these two states remain very small. Only around 15% through state $|2\rangle$ at $t = 55$ fs and less than 10% through state $|3\rangle$ at $t = 60$ fs, we refer evidently here to the two peaks in Fig 11(b). The optimized pulses generated from the four-level system by using the

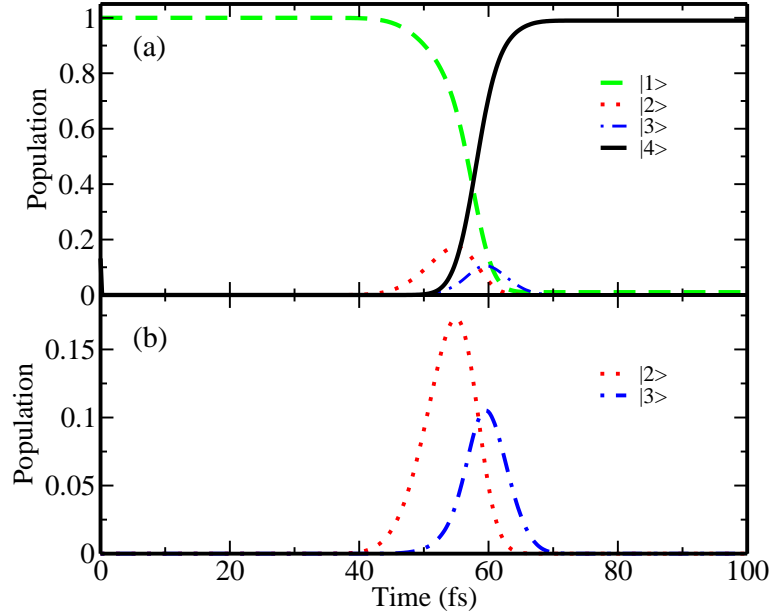


Figure 11. The population evolution in a four level system with a sequential coupling. Panel (a) shows the population transfer from the initial state $|1\rangle$ (green dashed curve) to the final state $|4\rangle$ (solid black line). Panel (b) is displaying the population evolution of the intermediate states $|2\rangle$ (red dotted curve) and $|3\rangle$ (blue dot-dashed curve).

new OCT method are presented in Fig. 12. One should remind that in this case we need three pulses; the pump to link the level $|1\rangle$ to level $|2\rangle$, the Stokes to link level $|3\rangle$ to level $|4\rangle$ and the third pulse which we call the intermediate pulse to link the two intermediate levels $|2\rangle$ and $|3\rangle$. As in the three-level system, we obtain automatically the counterintuitive mechanism. One can see clearly the pump pulse (solid black line) precedes the Stokes pulse (dashed red line). Nevertheless we observe the intermediate pulse Ω_I overlaps both the Stokes and the pump pulses. This phenomena is quite equivalent to the one obtained from the local optimization (14), where indeed the envelope of the intermediate pulse straddle the Stokes and the pump, yet with a higher intensity. In reference (14), authors attributed to this pattern the name of *straddling* STIRAP sequence (S-STIRAP) and demonstrated that is a robust extension of STIRAP to multilevel systems. They illustrated indeed the applicability of this method to five- and nine-level systems. Since the new OCT method leads to equivalent results for three- and four-level systems, we expect that it would conduct to similar conclusion for N -level systems.

4. CONCLUSION

With reference to Tannor’s work (14) we have shown that STIRAP-type solution can be generated from an OCT calculation. To obtain this solution, a state-dependent constraint has been added to the objective functional. Comparisons with STIRAP in a Λ -type three-level system have shown that this new OCT formulation leads to equivalent population transfers with a minimum of loss in forbidden levels for same initial energies. In addition, it has proven itself to generate slightly better population transfer when we have pulse fluctuations introduced into the system. However STIRAP appears to be slightly more robust with respect to the decay of the intermediate

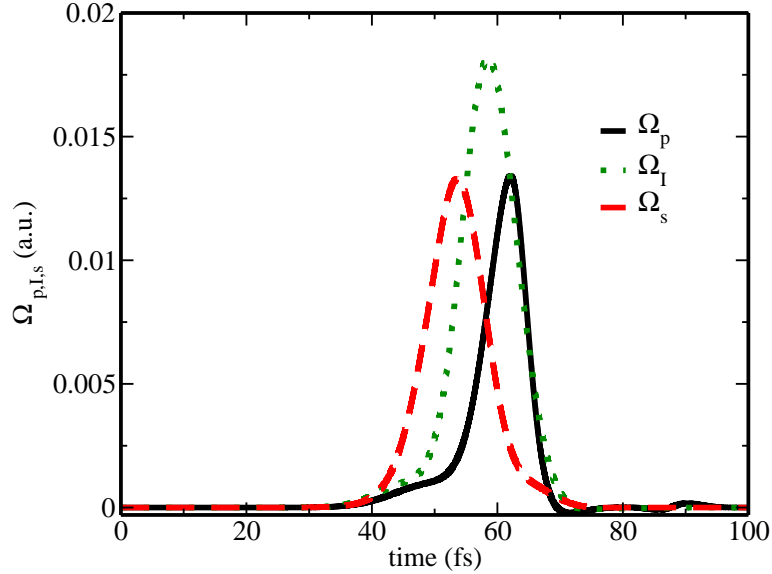


Figure 12. The sequence of the optimized pulses in a sequentially coupled four-level system. The pump pulse is presented in solid black line, the Stokes in dashed red line. The intermediate pulse which couple the two intermediate levels $|2\rangle$ and $|3\rangle$ is presented by the dotted green line. Note here that the counterintuitive sequence of the pump pulse preceded by the Stokes is generated automatically. We remark also the intermediate pulse overlaps the two other pulses and its intensity is much higher comparing to the intensities of the Stokes and the pump. This phenomena was obtained in the past by using LCT calculation and was called "straddling" STIRAP.

forbidden state. Furthermore the advantage of using this new method is the fact that it could be extended from a three-level system to multilevel systems.

Acknowledgment(s)

The authors would like to thank Prof. Christiane Koch her helpful discussions.

References

References

- (1) Marlan O. Scully and M. Suhail Zubairy, *Quantum Optics* (Cambridge University Press, New York, (1997)).
- (2) K. Bergmann, H. Theuer and B. W. Shore, *Reviews of Modern Physics* 70 (1998) 1003.
- (3) U. Gaubatz, P. Rudecki, S. Schiemann and K. Bergmann, *Journal of Chemical Physics* 92 (1990) 5363.
- (4) N. V. Vitanov, T. Halfmann, B. Shore, K. Bergmann, *Annual Review of Physical Chemistry* 52 (2001) 763.
- (5) M. P. Fewell, B. W. Shore and K. Bergmann, *Australian Journal of Physics* 50 (1997) 281.
- (6) M. Fleischhauer and Aaron S. Manka, *Physical Review A* 54 (1996) 794.
- (7) M. N. Kobrak and S. A. Rice, *Physical Review A* 57 (1998) 1158.
- (8) Y. B. Band and O. Magner, *Physical Review A* 50 (1994) 584.
- (9) M. Elk, *Physical Review A* 52 (1995) 4017.

- (10) S. Schiemann, A. Kuhn, S. Steuerwald and K. Bergmann, *Physical Review Letters* 71 (1993) 3637.
- (11) A. Jaouadi, E. Barrez, Y. Justum and M. Desouter-Lecomte, *Journal of Chemical Physics* 139 (2103) 014310
- (12) J. R. Kuklinski, U. Gaubatz, F. T. Hioe and K. Bergmann, *Physical Review A* 40 (1989) 6741.
- (13) S. Guérin, H. R. Jauslin, *Advances in Chemical Physics* 125 (2003) 147.
- (14) V. S. Malinovsky and D. J. Tannor, *Physical Review A* 56 (1997) 4929.
- (15) D. J. Tannor, R. Kosloff and A. Bartana, *Faraday Discussions* 113 (1999) 365.
- (16) H. Yuan, C. P. Koch, P. Salamon and D. J. Tannor, *Physical Review A* 85 (2012) 033417.
- (17) J. P. Palao, R. Kosloff and C. P. Koch, *Physical Review A* 77 (2008) 063412.
- (18) M. M. Müller, D. M. Reich, M. Murphy, H. Yuan, J. Vala, K. B. Whaley, T. Calarco and C. P. Koch, *Physical Review A* 84 (2011) 042315.
- (19) Y. Ohtsuki, G. Turicini, H. Rabitz, *Journal of Chemical Physics* 120 (2004) 5509.
- (20) K. Sundermann, R. de Vivie-Riedle, *Journal of Chemical Physics* 110 (1999) 1896.
- (21) M. V. Ammosov, N. B. Delone and V. P. Krainov, *Soviet Physics. Journal of Experimental and Theoretical Physics* 64 (1986) 1191.
- (22) W. Zhu, J. Botina, H. Rabitz, *Journal of Chemical Physics* 108 (1998) 1953.
- (23) J. P. Palao and R. Kosloff, *Physical Review A* 68 (2003) 062308.
- (24) M. Ndong, H. Tal-Ezer, R. Kosloff, C. P. Koch, *Journal of Chemical Physics* 130 (2009) 124108.
- (25) D. J. Tannor, V. Kazakov, and V. Orlov, *Time Dependent Quantum Molecular Dynamics* (1992) 347.
- (26) J. Somlo, V. A. Kazakov and D. J. Tannor, *Chemical Physics* 172 (1993) 85.